J. Fluid Mech. (2003), *vol.* 486, *pp.* 1–20. © 2003 Cambridge University Press
DOI: 10.1017/S0022112003004312 Printed in the United Kingdom

The behaviour of a particle in orthogonal acoustic fields

By A. Y. REDNIKOV[1], N. RILEY[2] AND S. S. SADHAL[1]

[1]Department of Aerospace and Mechanical Engineering, University of Southern California, Los Angeles, CA 90089-1453, USA

[2]School of Mathematics, University of East Anglia, Norwich NR4 7TJ, UK

(Received 20 September 2000 and in revised form 14 May 2002)

We are concerned with the response of an unconstrained particle, solid or liquid, placed in an acoustic field which consists of two orthogonal sound waves. These have the same amplitude and wavenumber, but differ in phase by $\pi/2$. The particle may be either a circular cylinder or a sphere. The effect of the superimposed waves is to create a time-averaged torque on the particle which causes it to rotate with uniform angular velocity. Throughout, a suitably defined Strouhal number is assumed to be large, with the solution developed in appropriate inverse powers of it. The particle size is assumed to be much smaller than the acoustic wavelength. At leading order it is shown that solid and liquid cylinders behave in a similar manner, in the sense that the liquid is in solid-body rotation. For a spherical liquid drop, the dominant time-averaged motion of it is also a solid-body rotation when the drop viscosity is large compared with that of the fluid environment; however, superposed on this is a time-averaged recirculatory flow within the droplet in the form of a pair of toroidal vortices.

1. Introduction

In an earlier paper Riley (1966) considered the steady streaming about a spherical solid particle in an oscillating environment. If that environment results from an acoustic wave, the particle is assumed to be at a pressure node. Zhao, Sadhal and Trinh (1999*b*) and Yarin *et al.* (1999) extend this work to the case of a liquid droplet within which there is now an induced time-independent circulation. The effects of compressibility in the gaseous environment have been included by Lee & Wang (1990), Zhao *et al.* (1999*a*) and Yarin *et al.* (1999) in the case when a solid particle or droplet is located between a velocity node and antinode.

In the present paper we locate a particle, which may be either a circular cylinder or a sphere, liquid or solid, at a pressure node in the acoustic field associated with two orthogonal sound waves. To enable this physically we may suppose either that the particle is in a low-gravity environment or, if it is in earth gravity, levitated electrostatically, as in the experiments of Rhim, Chung & Elleman (1988), with the orthogonal sound waves in a horizontal plane. The sound pressure amplitude of the two waves is the same, but their phase differs by $\pi/2$. Lee & Wang (1989) and Riley (1992) have considered this situation for a fixed solid sphere and cylinder, respectively, generalized to allow for different sound pressure amplitudes, and have shown that a torque is induced by the streaming. In the present investigation we allow the particles

https://doi.org/10.1017/S0022112003004312 Published online by Cambridge University Press

to rotate freely and, for the case of liquid particles, we also consider the flow within the liquid phase.

The plan of the paper is as follows. In § 2, we introduce the equations of motion, and in particular identify the two parameters that characterize the flow. If U_0 and ω are the velocity amplitude and frequency of the oscillatory flow, respectively, and if a is a typical length, say the radius of cylinder or sphere, with ν the kinematic viscosity of the fluid environment, then we have $\epsilon = U_0/\omega a$, the inverse Strouhal number, as a small parameter. For the second parameter, it is convenient to take a Reynolds number of the time-averaged flow that develops, see Riley (1967). In the papers cited above this is seen to be $R_s = U_0^2/\omega\nu$. However, in the more complex situation which we deal with here, we argue that the appropriate streaming Reynolds number is now $\tilde{R}_s = U_0^2 a/(\omega\nu^3)^{1/2}$. This is followed in § 3 by the case of a circular cylinder. A time-independent flow is induced by the action of the Reynolds stresses within the Stokes shear-wave layer, and the torque provided by this causes the cylinder to rotate. The rotation rate increases with $\tilde{R}_s$, to the extent that the speed at the cylinder surface may be far in excess of U_0. The analysis is closely similar for a liquid cylinder, and in particular it is shown that since the Reynolds stresses in the Stokes layer at the interface are negligibly small in the liquid phase, for a typical liquid–gas system, the fluid motion is, at leading order, simply a solid-body rotation.

In § 4 we consider the analogous situation for a spherical particle. Again, we first consider the case of a solid sphere. Rotation of the sphere is again induced, but the flow is now more complex. For the rotating circular cylinder, the flow outside the Stokes layer is simply that due to a line vortex independent of Reynolds number. For a rotating sphere, the flow characteristics change with Reynolds number. The flow due to a steadily rotating sphere has been considered by Takagi (1977) for small Reynolds numbers, Dennis, Ingham & Singh (1981) for $O(1)$ Reynolds numbers and Banks (1976) for large Reynolds numbers. We have been able to exploit their results to calculate the rotation rate of the sphere. In particular, and in contrast to the cylindrical flow, we find that speeds are always small compared with U_0. For the case of a liquid drop, the flow within it is again dominated by solid-body rotation. However, unlike the case of a liquid cylinder there is, now, superposed on this a recirculating flow within it which, for small values of $\tilde{R}_s$, takes the form of two toroidal vortices, whose common axis coincides with the axis of rotation of the sphere. For both solid and liquid spheres we have determined corrections to the steady streaming outside the drop, and in particular shown how this is influenced by drop liquidity. These results enable us to make interesting comparisons with the earlier works cited above. In particular, we show that in many situations there are identical flow structures, but for a change in sign; and for the case of a liquid particle an unexpected flow reversal may take place which results in a recirculating flow beyond the Stokes layer outside the drop.

The acoustic context in which we have introduced our investigation has limitations. In particular, we treat the fluids as incompressible fluids. The implication of this is that if k is the wavenumber then $ka \ll 1$. However, our analysis does have wider applicability. There are examples of the applications of our theory that are not directly related to acoustics. As an example consider a particle, free to rotate, which is driven in a high-frequency small-amplitude orbital motion in an incompressible fluid which is otherwise at rest. With axes fixed, in a non-rotating frame, at the particle the observed flow is identical with the above acoustic case. The common feature of these two examples is that the fluid environment and the particle perform an orbital oscillation relative to one another.

https://doi.org/10.1017/S0022112003004312 Published online by Cambridge University Press

2. Governing equations

We consider a situation in which either a cylindrical or spherical particle and the incompressible fluid environment perform small-amplitude high-frequency circular orbital oscillations relative to one another. Such an oscillation is a superposition of two orthogonal axial oscillations which have the same amplitude but differ in phase by $\pi/2$. Two examples of such motions are described in § 1. In the present paper, we consider the case in which the particles are unconstrained in the sense that they are free to rotate. From geometrical considerations, rotation about an axis perpendicular to the orbital plane may be anticipated. Furthermore, the rotation is expected to be purely steady; self-induced torsional oscillations are discarded by symmetry considerations. Our analysis is carried out in the non-rotating reference frame fixed to the particle. In the case of liquid particles we limit our consideration to the situation in which the coefficient of viscosity of the particle is large compared with the host fluid.

The equations of motion governing the flow are

$$\frac{\partial \boldsymbol{v}'}{\partial t'} - \boldsymbol{v}' \wedge (\nabla \wedge \boldsymbol{v}') = -\frac{1}{\rho}\nabla\left(p' + \tfrac{1}{2}\rho \boldsymbol{v}'^2\right) - \nu \nabla \wedge \nabla \wedge \boldsymbol{v}', \quad \nabla \cdot \boldsymbol{v}' = 0. \tag{1}$$

At large distances from the particle we require

$$\boldsymbol{v}' \sim U_0 \cos \omega t' \boldsymbol{i} - U_0 \sin \omega t' \boldsymbol{j} \qquad \text{as} \quad |\boldsymbol{x}'| \to \infty. \tag{2}$$

In these equations t' is the time, ω the frequency, $\boldsymbol{v}'$ the velocity, p' the pressure (which absorbs the inertial force, if any), $\boldsymbol{x}'$ the position vector, ρ the fluid density and ν its kinematic viscosity, $\boldsymbol{i}$ and $\boldsymbol{j}$ are two orthogonal unit vectors.

Boundary conditions at the particle surface require the non-penetration and no-slip conditions to be satisfied for a solid particle, or non-penetration and continuity of velocity and stresses for a liquid particle. In addition, for the case of a solid particle, we require the net torque to vanish, which provides a condition on the angular velocity Ω' of the particle. We note that the angular velocity vector is then given by $\Omega' \boldsymbol{k}$, where $\boldsymbol{k} = \boldsymbol{i} \wedge \boldsymbol{j}$.

To introduce dimensionless variables we choose a as a length scale, ω^{-1} a time and the velocity amplitude U_0 of the sound waves as a velocity so that

$$\boldsymbol{x}' = a\boldsymbol{x}, \quad t' = t/\omega, \quad \boldsymbol{v}' = U_0 \boldsymbol{v}, \quad p' = \rho a \omega U_0 p, \quad \Omega' = U_0 \Omega / a, \tag{3}$$

and equations (1) and (2) become

$$\frac{\partial \boldsymbol{v}}{\partial t} + \epsilon\left\{\nabla\left(\tfrac{1}{2}\boldsymbol{v}^2\right) - \boldsymbol{v} \wedge (\nabla \wedge \boldsymbol{v})\right\} = -\nabla p - \frac{1}{M^2}\nabla \wedge \nabla \wedge \boldsymbol{v}, \quad \nabla \cdot \boldsymbol{v} = 0, \tag{4}$$

$$\boldsymbol{v} \sim \cos t \ \boldsymbol{i} - \sin t \ \boldsymbol{j} \quad \text{as} \quad |\boldsymbol{x}| \to \infty. \tag{5}$$

The two parameters that characterize the flow under consideration are introduced in (4) as

$$\epsilon = U_0/\omega a, \quad M^2 = \omega a^2/\nu.$$

The parameter ϵ is recognized as the inverse of a Strouhal number and is assumed small throughout. With $\epsilon \ll 1$, the amplitude of oscillation of fluid particles is small compared with the body scale. The frequency parameter M^2 is assumed to be large, and may be interpreted as a high-frequency limit. With $M^2 \gg 1$, the small-amplitude oscillatory flow is irrotational in the main body of the fluid; vorticity is generated in a thin shear-wave layer of thickness $O(a/M)$, the Stokes layer, at the body surface. The role of the Stokes layer is to enable the no-slip condition to be satisfied, and it is

https://doi.org/10.1017/S0022112003004312 Published online by Cambridge University Press

therefore characterized by large normal gradients of the tangential velocity, that are $O(M)$ times greater than in the main body of the fluid.

The two parameters ϵ and M are formally independent. One of our principal concerns in the present paper is to investigate the time-averaged flow, or steady streaming flow that develops within the oscillatory flow framework. The equation that governs this flow, namely the steady Navier–Stokes equation, which arises in our asymptotic development, will be of the most general form when the Reynolds number associated with it is $O(1)$. This parameter depends, as we shall see, upon both ϵ and M. To express it in terms of ϵ and M, we must determine the order of magnitude of the induced steady streaming. It is well known, see for example Riley (1966), that a steady streaming originates in the Stokes layer, owing to the action of the time-averaged Reynolds stresses that act therein. This streaming, with velocities $O(\epsilon U_0)$, is fully structured within the Stokes layer, but is not confined within it. The steady streaming persists at the edge of the Stokes layer where it drives a steady flow in the main body of the fluid with velocities $O(\epsilon U_0)$. A Reynolds number based on this, namely $R_s = \epsilon U_0 a/\nu = \epsilon^2 M^2$, is the appropriate streaming Reynolds number, as adopted by Riley (1966). The above argument relates to the classical situation in which a particle is fixed in the sound field. The situation under consideration here is different. Our particles, namely circular cylinders or spheres, are free to rotate whenever a net steady torque is created. That we may anticipate such a torque follows at once from the work of Lee & Wang (1989) and Riley (1992). For a steady rotation of the particle to result, there must be a balance between the viscous torque due to the structured steady flow component in the Stokes layer and that due to the global steady flow caused by particle rotation. In the Stokes layer, the velocity of the structured flow is $O(\epsilon U_0)$, the normal length scale therein is $O(M)$ smaller than that of the flow due to steady rotation. Consequently, the velocity scale associated with rotation, which must differ in inverse proportion, is $O(\epsilon M U_0)$. A Reynolds number based on this velocity is $\epsilon M U_0 a/\nu = \epsilon^2 M^3$, and serves as our streaming Reynolds number. Accordingly, we define

$$\tilde{R}_s = \epsilon^2 M^3.$$

In the treatment that follows, ϵ and $\tilde{R}_s$ are our two independent parameters and, unless otherwise stated, $\tilde{R}_s = O(1)$.

For a liquid particle, additional parameters are involved. If μ and $\hat{\mu}$ are the coefficients of viscosity outside and within the particle, respectively, then $\delta_\mu = \mu/\hat{\mu}$ will be an important parameter. We shall be concerned with the case $\delta_\mu \ll 1$ for which a liquid drop in a gaseous environment is an example. In particular, we shall see advantage in taking $\delta_\mu = O(\epsilon^{2/3}\tilde{R}_s^{-1/3})$ so that $M_\mu = M\delta_\mu \equiv \epsilon^{-2/3}\tilde{R}_s^{1/3}\delta_\mu$ is an $O(1)$ quantity. The ratio of the kinematic viscosities, $\delta_\nu = \nu/\hat{\nu}$, is formally treated as an $O(1)$ quantity.

The velocity and pressure fields are represented as

$$\boldsymbol{v} = \boldsymbol{v}^{(1)}\mathrm{e}^{\mathrm{i}t} + \epsilon\boldsymbol{v}^{(0)} + \sum_{n=2}^{\infty}\epsilon^{n-1}\boldsymbol{v}^{(n)}\mathrm{e}^{\mathrm{i}nt}, \tag{6}$$

$$p = p^{(1)}\mathrm{e}^{\mathrm{i}t} + \epsilon p^{(0)} + \sum_{n=2}^{\infty}\epsilon^{n-1}p^{(n)}\mathrm{e}^{\mathrm{i}nt}. \tag{7}$$

The steady part and the higher-order harmonics are generated by means of nonlinearity, and accordingly involve progressively higher powers of ϵ. Each complex

https://doi.org/10.1017/S0022112003004312 Published online by Cambridge University Press

amplitude on the right-hand sides of (6) and (7) is a function of the spatial coordinates and does not depend on the time. As usual in such cases, only the real part is intended.

Each term in (6) and (7) is in turn represented as

$$\boldsymbol{v}^{(0)} = \sum_{m=-1}^{\infty} \left(\frac{\epsilon^{2/3}}{\tilde{R}_s^{1/3}}\right)^m \boldsymbol{v}_m^{(0)}, \quad \boldsymbol{v}^{(n)} = \sum_{m=0}^{\infty} \left(\frac{\epsilon^{2/3}}{\tilde{R}_s^{1/3}}\right)^m \boldsymbol{v}_m^{(n)}, \quad p^{(n)} = \sum_{m=0}^{\infty} \left(\frac{\epsilon^{2/3}}{\tilde{R}_s^{1/3}}\right)^m p_m^{(n)}, \quad (8a\text{–}c)$$

where $n = 1, 2\ldots$ in (8*b*), and $n = 0, 1\ldots$ in 8(*c*). In (8) the series expansions are essentially in powers of M^{-1}, as developed by Riley (1967) where it is replaced by $\epsilon/R_s^{1/2}$ for $R_s = O(1)$, in our case as already argued, we have $\tilde{R}_s = O(1)$, and thus M^{-1} is replaced by $\epsilon^{2/3}/\tilde{R}_s^{1/3}$. The only departure from the general scheme can be observed in $\boldsymbol{v}^{(0)}$, where a term corresponding to $m = -1$ is foreseen in accordance with the earlier argument, and is due to the fact that the particle is free to rotate.

As already mentioned, no torsional oscillations are expected in the present problem, therefore Ω is time-independent. Then corresponding to the time-independent terms in (6) and (8) we have

$$\Omega = \epsilon\, \Omega^{(0)}, \quad \Omega^{(0)} = \sum_{m=-1}^{\infty} \left(\frac{\epsilon^{2/3}}{\tilde{R}_s^{1/3}}\right)^m \Omega_m^{(0)}. \tag{9}$$

The representation (6)–(9) serves to establish the structure of the expansion with the smallness parameter. Subsequently, whilst making use of this structure, we find it convenient to express variables as single series in powers of $\epsilon^{1/3}$, which involves a slight change of notation.

3. The circular cylinder

3.1. *A solid cylinder*

The cylinder has radius a, and for this two-dimensional problem it is convenient to work in polar coordinates (r, θ) with $x = r\cos\theta$, $y = r\sin\theta$, $\boldsymbol{v} = (v_r, v_\theta)$, and introduce the stream function ψ such that $v_r = r^{-1}\partial\psi/\partial\theta$, $v_\theta = -\partial\psi/\partial r$. With the pressure eliminated from (4), we then have

$$\frac{\partial}{\partial t}(\nabla^2\psi) - \frac{\epsilon}{r}\frac{\partial(\psi, \nabla^2\psi)}{\partial(r,\theta)} = \frac{\epsilon^{4/3}}{\tilde{R}_s^{2/3}}\nabla^4\psi, \tag{10}$$

with

$$\psi = 0, \quad \frac{\partial\psi}{\partial r} = -\Omega \quad \text{at} \quad r = 1,$$

and

$$\psi \sim -\mathrm{i}r\mathrm{e}^{\mathrm{i}(\theta+t)} \quad \text{as} \quad r \to \infty.$$

Here and throughout, the real part of any complex quantity is to be understood. The conditions at $r = 1$ anticipate the rotation of the cylinder with angular velocity Ω.

We now expand the streamfunction ψ in a manner analogous to (6) and (8). We have

$$\begin{aligned}\psi = {} & \{\psi_0^{(1)} + \epsilon^{2/3}\tilde{R}_s^{-1/3}\psi_1^{(1)} + \epsilon^{4/3}\tilde{R}_s^{-2/3}\psi_2^{(1)} + \ldots\}\mathrm{e}^{\mathrm{i}t} \\ & + \epsilon^{1/3}\tilde{R}_s^{1/3}\{\psi_{-1}^{(0)} + \epsilon^{2/3}\tilde{R}_s^{-1/3}\psi_0^{(0)} + \epsilon^{4/3}\tilde{R}_s^{-2/3}\psi_1^{(0)} + \ldots\} \\ & + \epsilon\{\psi_0^{(2)} + \epsilon^{2/3}\tilde{R}_s^{-1/3}\psi_1^{(2)} + \ldots\}\mathrm{e}^{2\mathrm{i}t} + \text{higher harmonics},\end{aligned}$$

https://doi.org/10.1017/S0022112003004312 Published online by Cambridge University Press

which we now find convenient to write as

$$\psi = \psi_0^{(u)} + \epsilon^{1/3}\tilde{R}_s^{1/3}\psi_1^{(s)} + \epsilon^{2/3}\tilde{R}_s^{-1/3}\psi_2^{(u)} + \epsilon\{\psi_3^{(s)} + \psi_3^{(u)}\} + \epsilon^{4/3}\tilde{R}_s^{-2/3}\psi_4^{(u)} + \epsilon^{5/3}\tilde{R}_s^{-1/3}\{\psi_5^{(s)} + \psi_5^{(u)}\} + O(\epsilon^2), \quad (11)$$

where superscripts (s), (u), denote 'steady' and 'unsteady' respectively, together with

$$\Omega = \epsilon^{1/3}\tilde{R}_s^{1/3}\Omega_1 + \epsilon\,\Omega_3 + O(\epsilon^{5/3}). \quad (12)$$

In rewriting the initial expansion, which is in terms of harmonic functions, in powers of $\epsilon^{1/3}$, we have found it convenient to introduce a change of notation. In particular, a superscript (s) denotes a term formally independent of t, a superscript (u) a term that depends upon t by the inclusion of the appropriate harmonics, and the subscript relates to the appropriate power of $\epsilon^{1/3}$.

Substituting (11) into (10) gives, at leading order,

$$\frac{\partial}{\partial t}(\nabla^2\psi_0^{(u)}) = 0,$$

from which we infer that $\nabla^2\psi_0^{(u)} = 0$ and so

$$\psi_0^{(u)} = -\mathrm{i}\left(r - \frac{1}{r}\right)\mathrm{e}^{\mathrm{i}(\theta+t)}. \quad (13)$$

This does not satisfy the condition of no slip at $r = 1$, and to accommodate that we introduce the Stokes-layer variables

$$\Psi = \frac{\tilde{R}_s^{1/3}}{\sqrt{2}}\frac{\psi}{\epsilon^{2/3}}, \qquad \eta = \frac{\tilde{R}_s^{1/3}}{\sqrt{2}}\frac{(r-1)}{\epsilon^{2/3}}. \quad (14)$$

Upon substituting these into (10), and retaining the leading-order linear and nonlinear terms, we obtain

$$\frac{\partial}{\partial t}\left(\frac{\partial^2\Psi}{\partial\eta^2}\right) - \epsilon\frac{\partial(\Psi, \partial^2\Psi/\partial\eta^2)}{\partial(\eta,\theta)} = \frac{1}{2}\frac{\partial^4\Psi}{\partial\eta^4}. \quad (15)$$

As in (11), we expand the solution of (15) as

$$\Psi = \Psi_0^{(u)} + \epsilon^{1/3}\tilde{R}_s^{1/3}\Psi_1^{(s)} + \epsilon^{2/3}\tilde{R}_s^{-1/3}\Psi_2^{(u)} + \epsilon\{\Psi_3^{(s)} + \Psi_3^{(u)}\} + O(\epsilon^{4/3}). \quad (16)$$

At leading order we have

$$\frac{\partial}{\partial t}\left(\frac{\partial^2\Psi_0^{(u)}}{\partial\eta^2}\right) = \frac{1}{2}\frac{\partial^4\Psi_0^{(u)}}{\partial\eta^4}. \quad (17)$$

The solution of (17) that satisfies $\Psi_0^{(u)} = 0$ and the no-slip condition $\partial\Psi_0^{(u)}/\partial\eta = 0$ at $\eta = 0$ is, upon matching with (13),

$$\Psi_0^{(u)} = -2\mathrm{i}\left[\eta - \tfrac{1}{2}(1-\mathrm{i})\{1 - \mathrm{e}^{-(1+\mathrm{i})\eta}\}\right]\mathrm{e}^{\mathrm{i}(\theta+t)}.$$

From (15), (16) we see that at $O(\epsilon^{1/3})$ we have $\partial^4\Psi_1^{(s)}/\partial\eta^4 = 0$ from which we deduce that

$$\Psi_1^{(s)} = -\Omega_1\eta. \quad (18)$$

Returning to the outer solution, the terms $O(\epsilon^{n/3})$ and $n = 2, 3$ yield simply $\nabla^2\psi_n^{(u)} = 0$, the solutions of which are not needed. The terms $O(\epsilon^{4/3})$ and $O(\epsilon^{5/3})$ yield,

https://doi.org/10.1017/S0022112003004312 Published online by Cambridge University Press

respectively,

$$\left.\begin{aligned}\frac{\partial}{\partial t}\left(\nabla^2\psi_4^{(u)}\right)-\frac{\tilde{R}_s}{r}\frac{\partial\left(\psi_0^{(u)},\nabla^2\psi_1^{(s)}\right)}{\partial(r,\theta)}&=0,\\ \frac{\partial}{\partial t}\left(\nabla^2\psi_5^{(u)}\right)-\frac{\tilde{R}_s}{r}\frac{\partial\left(\psi_1^{(s)},\nabla^2\psi_1^{(s)}\right)}{\partial(r,\theta)}&=\nabla^4\psi_1^{(s)}.\end{aligned}\right\}\tag{19}$$

If we now take a time-average of equation (19), we find that $\psi_1^{(s)}$ satisfies

$$-\frac{1}{r}\frac{\partial\left(\psi_1^{(s)},\nabla^2\psi_1^{(s)}\right)}{\partial(r,\theta)}=\frac{1}{\tilde{R}_s}\nabla^4\psi_1^{(s)},\tag{20}$$

which we identify as the steady Navier–Stokes equation with $\tilde{R}_s$ as Reynolds number. Equation (20) is satisfied by taking $\nabla^2\psi_1^{(s)}=0$, and we obtain the solution matching with (18) as

$$\psi_1^{(s)}=-\Omega_1\ln r.\tag{21}$$

We note that $\psi_1^{(s)}$ in equation (21) is a uniformly valid solution which satisfies all the conditions at $r=1$ although Ω_1 is, as yet, undetermined. Our main interest lies with the time-averaged flow and we move next to the terms $O(\epsilon)$ in the Stokes layer. From (15) and (16) we see that when these are time-averaged we have

$$-\frac{1}{2}\frac{\partial^4\Psi_3^{(s)}}{\partial\eta^4}=\left\langle\frac{\partial\left(\Psi_0^{(u)},\partial^2\Psi_0^{(u)}/\partial\eta^2\right)}{\partial(\eta,\theta)}\right\rangle,\tag{22}$$

where $\langle.\rangle$ denotes a time average, with

$$\Psi_3^{(s)}=0,\quad \frac{\partial\Psi_3^{(s)}}{\partial\eta}=-\Omega_3\quad\text{at}\quad\eta=0,$$

and

$$\Psi_3^{(s)}\sim\frac{\Omega_1}{\sqrt{2}}\eta^2\quad\text{as}\quad\eta\to\infty,$$

to ensure matching with the outer solution. The required solution is

$$\Psi_3^{(s)}=-\Omega_3\eta+\frac{\Omega_1}{\sqrt{2}}\eta^2+3\eta-\tfrac{3}{2}+2\eta\mathrm{e}^{-\eta}\cos\eta+2\mathrm{e}^{-\eta}\cos\eta-4\mathrm{e}^{-\eta}\sin\eta-\tfrac{1}{2}\mathrm{e}^{-2\eta},\tag{23}$$

with Ω_3 undetermined at this stage.

Now, with the steady flow in the Stokes layer given by (16), (18) and (23), we are in a position to calculate the net torque on the cylinder, which is found to be

$$\Gamma=-2\sqrt{2}\pi(\sqrt{2}\Omega_1+1).\tag{24}$$

We note that the dimensional value of the torque is restored by multiplying (24) by $\rho U_0^2a^2\epsilon^{2/3}\tilde{R}_s^{-1/3}$.

Since a steady rotation of the cylinder requires that the net torque on it vanishes, we have

$$\Omega_1=-\frac{1}{\sqrt{2}}.\tag{25}$$

This corresponds to a clockwise rotation of the cylinder. We note from equation (5) that fluid particles at large distances move on circles of radius ϵa in the same

https://doi.org/10.1017/S0022112003004312 Published online by Cambridge University Press

clockwise direction, but at a much greater rate than the cylinder rotation, of course. When rewritten in terms of the original Ω from (12), the result (25) becomes

$$\Omega = -\frac{(\epsilon \tilde{R}_s)^{1/3}}{\sqrt{2}}. \tag{26}$$

The steady Navier–Stokes equation, (20), has emerged from our formal analysis with $\tilde{R}_s = O(1)$. However, the line vortex solution, (21), is independent of $\tilde{R}_s$ which suggests that, in principle, the rotation rate, (26), may increase indefinitely with $\tilde{R}_s$, despite the smallness of ϵ. However, inspection of equation (15) shows that for $|\Omega| = O(\epsilon^{-1})$, which corresponds to $\tilde{R}_s = O(\epsilon^{-4})$, there is a nonlinear interaction between the steady rotation and the primary oscillatory flow. This distinguished limit, $\tilde{R}_s = O(\epsilon^{-4})$, which we study in more detail below, may place an upper bound on the applicability of (26).

We write

$$\tilde{R}_s = \alpha_s \epsilon^{-4}, \tag{27}$$

in equation (10). Taking account of (11), (13), (21) and (27), it is appropriate to expand ψ as

$$\psi = \epsilon^{-1}\overline{\Omega}_{-1} \ln r - \mathrm{i}\left(r - \frac{1}{r}\right)\mathrm{e}^{\mathrm{i}(\theta+t)} + O(\epsilon),$$

while the counterpart of (12) is now

$$\Omega = \epsilon^{-1}\overline{\Omega}_{-1} + O(\epsilon). \tag{28}$$

In order to accommodate the no-slip condition at $r = 1$, the Stokes-layer thickness is now $O(\epsilon^2)$ and (14) is replaced by

$$\Psi = \frac{\alpha_s^{1/3}}{\sqrt{2}}\frac{\psi}{\epsilon^2}, \qquad \eta = \frac{\alpha_s^{1/3}}{\sqrt{2}}\frac{(r-1)}{\epsilon^2},$$

which again leads to equation (15) as the equation for Ψ. In the Stokes layer, we now write

$$\Psi = -\epsilon^{-1}\overline{\Omega}_{-1}\eta + \Psi_0^{(u)} + \epsilon\left\{\Psi_1^{(s)} + \Psi_1^{(u)}\right\} + O(\epsilon^2).$$

The leading terms of (15) now give

$$\frac{\partial}{\partial t}\left(\frac{\partial^2 \Psi_0^{(u)}}{\partial \eta^2}\right) + \overline{\Omega}_{-1}\frac{\partial^3 \Psi_0^{(u)}}{\partial \theta \partial \eta^2} = \frac{1}{2}\frac{\partial^4 \Psi_0^{(u)}}{\partial \eta^4}; \tag{29}$$

and when (29) is compared with equation (17) we see that the limit represented by (27) that we have adopted is 'distinguished' in the sense that for such large $\tilde{R}_s$, convective terms now appear at leading order in the time-dependent flow. The solution of (29) which satisfies $\Psi_0^{(u)} = \partial \Psi_0^{(u)}/\partial \eta = 0$ at $\eta = 0$, with $\Psi_0^{(u)} \sim -2\mathrm{i}\eta \mathrm{e}^{\mathrm{i}(\theta+t)}$ as $\eta \to \infty$, is

$$\Psi_0^{(u)} = -\frac{2\mathrm{i}}{|\lambda|^{1/2}}\left[\xi - \tfrac{1}{2}\left\{1 - \mathrm{i}\,\mathrm{sgn}(\lambda)\right\}\left\{1 - \mathrm{e}^{-(1+\mathrm{i}\,\mathrm{sgn}(\lambda))\xi}\right\}\right]\mathrm{e}^{\mathrm{i}(\theta+t)},$$

where $\xi = |\lambda|^{1/2}\eta$ with $\lambda = 1 + \overline{\Omega}_{-1}$. If we now turn to the time-independent quantity $\Psi_1^{(s)}$ we see that, rather than (22), this now satisfies

$$\frac{1}{2}\frac{\partial^4 \Psi_1^{(s)}}{\partial \xi^4} = -\frac{1}{|\lambda|^{1/2}}\left\langle \frac{\partial\left(\Psi_0^{(u)}, \partial^2 \Psi_0^{(u)}/\partial \xi^2\right)}{\partial(\xi, \theta)} \right\rangle$$

https://doi.org/10.1017/S0022112003004312 Published online by Cambridge University Press

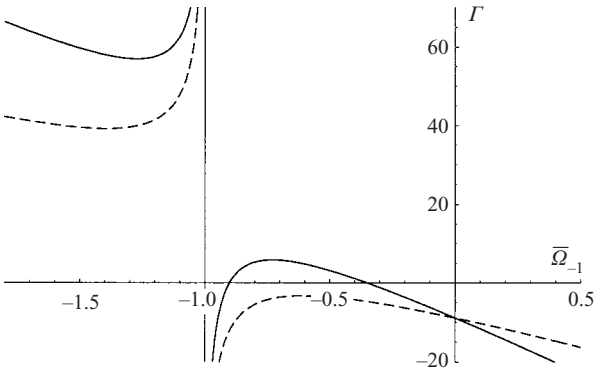


FIGURE 1. Torque on the cylinder *vs.* the rotation rate, equation (30). The solid line corresponds to $\alpha_s^{1/3} = 0.4$ whilst the dashed one to $\alpha_s^{1/3} = 0.7$. We note that for an unconstrained cylinder the rotation rate is determined from $\Gamma = 0$.

with, in addition to the non-penetration and no-slip condition at $\xi = 0$, the matching condition

$$\Psi_1^{(s)} \sim \frac{\alpha_s^{-1/3}}{\sqrt{2}} \frac{\overline{\Omega}_{-1}}{|\lambda|} \xi^2 \quad \text{as} \quad \xi \to \infty.$$

The solution is

$$\Psi_1^{(s)} = \frac{\alpha_s^{-1/3}}{\sqrt{2}} \frac{\overline{\Omega}_{-1}}{|\lambda|} \xi^2 - \frac{\overline{\Omega}_1}{|\lambda|^{1/2}} \xi + \frac{\operatorname{sgn}(\lambda)}{|\lambda|^{3/2}} \left(3\xi - \tfrac{3}{2} + 2\xi \mathrm{e}^{-\xi} \cos\xi + 2\mathrm{e}^{-\xi} \cos\xi - 4\mathrm{e}^{-\xi} \sin\xi - \tfrac{1}{2}\mathrm{e}^{-2\xi} \right)$$

which is similar to (23).

We are now able to calculate the torque on the cylinder. Recalling that $\lambda = 1 + \overline{\Omega}_{-1}$, we obtain

$$\Gamma = -2\sqrt{2}\pi \left\{ \frac{\operatorname{sgn}(1 + \overline{\Omega}_{-1})}{|1 + \overline{\Omega}_{-1}|^{1/2}} + \frac{\sqrt{2}}{\alpha_s^{1/3}} \overline{\Omega}_{-1} \right\}. \tag{30}$$

We can see that (24) is recovered from (30) in the limit $\alpha_s \to 0$, $\overline{\Omega}_{-1} \to \alpha_s^{1/3} \Omega_1$. Again, the net torque on the cylinder is to vanish, $\Gamma = 0$, which gives an equation for $\overline{\Omega}_{-1}$. The relation (30) is plotted in figure 1 for $\alpha_s^{1/3} = 0.4$ (the solid line) and $\alpha_s^{1/3} = 0.7$ (the dashed line). We see that if α_s is sufficiently small, namely $\alpha_s < \alpha_{sm}$ with $\alpha_{sm} = (2/3)^{9/2}$, the equation $\Gamma = 0$ has two roots. The one with the lower absolute value of $\overline{\Omega}_{-1}$ is the one that matches in the parameter space with the result obtained previously. Indeed, we have $\overline{\Omega}_{-1} \to -\alpha_s^{1/3}/\sqrt{2}$ as $\alpha_s \to 0$ which upon substitution into (28) coincides with (26). At $\alpha_s = \alpha_{sm}$ the two roots merge and for $\alpha_s > \alpha_{sm}$ the equation $\Gamma = 0$ has no solutions.

In view of what has been uncovered in relation to the number of steady states, it would be interesting to study the associated transient regimes of cylinder rotation. We shall not do it here in the general case. Rather, we shall assume that the cylinder is massive as compared to the surrounding fluid and therefore the time scale for the variation of the rotation rate is much greater than the viscous time scale in the fluid. In this case we can write $\mathrm{d}\overline{\Omega}_{-1}/\mathrm{d}\overline{t} = \Gamma(\overline{\Omega}_{-1})$, which is an evolution equation for $\overline{\Omega}_{-1}$. Here the right-hand side is given by (30) whilst $\overline{t}$ is the appropriately defined 'slow' time variable. Then we see immediately that, of the two regimes existing for

https://doi.org/10.1017/S0022112003004312 Published online by Cambridge University Press

$\alpha_s < \alpha_{sm}$, the one with the lower absolute value of $\overline{\Omega}_{-1}$ is stable (therefore, an attractor) while the other is unstable. Furthermore, we find that $\overline{\Omega}_{-1} = -1$ is another attractor of the evolution equation. We note that $\overline{\Omega}_{-1} = -1$ in fact corresponds to the resonance condition, when the cylinder rotation rate is equal to the frequency of primary oscillations. It is a singular point in our analysis, leading in particular to the vertical asymptote shown in figure 1. The singularity should be resolved within a refined asymptotic analysis for $\overline{\Omega}_{-1}$ in a small vicinity of $\overline{\Omega}_{-1} = -1$. However, we do not pursue this further here. Thus, for $\alpha_s < \alpha_{sm}$, there are actually two attractors of the evolution equation, and which one is attained depends on the initial condition. For $\alpha_s > \alpha_{sm}$, the resonant rotation $\overline{\Omega}_{-1} = -1$ remains the only attractor. On the other hand, in the limit $\alpha_s \to 0$ we note that the unstable regime approaches $\overline{\Omega}_{-1} = -1$. It would be natural to expect that it finally mutually annihilates with the resonant rotation regime so that only the regime with the lowest rotation rate remains. However, to study such an annihilation, if any, the aforementioned refined asymptotic approach is required and we do not pursue it here.

3.2. *A liquid cylinder*

Whilst a levitated rotating liquid cylinder may be subject to instabilities, and therefore difficult to realize in practice, it is nevertheless of interest to develop the solution for such a situation in view of what follows in § 4.

With $\hat{(.)}$ denoting a quantity in the liquid phase, the solution is constructed as in equations (11) and (12). In the gas phase then we have

$$\psi = -\mathrm{i}\left(r - \frac{1}{r}\right)\mathrm{e}^{\mathrm{i}(\theta+t)} - \epsilon^{1/3}\tilde{R}_s^{1/3}\Omega_1 \ln r + \ldots$$

and, with variables (14), the corresponding Stokes-layer solution is

$$\Psi = \left[-2\mathrm{i}\eta + A\left\{1 - \mathrm{e}^{-(1+\mathrm{i})\eta}\right\}\right]\mathrm{e}^{\mathrm{i}(\theta+t)} - \epsilon^{1/3}\tilde{R}_s^{1/3}\Omega_1\eta + \ldots,$$

where A is not yet determined. In the liquid phase, we introduce Stokes-layer variables as

$$\hat{\Psi} = \frac{\hat{R}_s^{1/3}}{\sqrt{2}}\frac{\hat{\psi}}{\epsilon^{2/3}}, \qquad \hat{\eta} = \frac{\hat{R}_s^{1/3}}{\sqrt{2}}\frac{(1-r)}{\epsilon^{2/3}} \quad \text{where} \quad \hat{R}_s = \epsilon^2\hat{M}^3.$$

The solution in the liquid Stokes layer is then

$$\hat{\Psi} = B\left\{1 - \mathrm{e}^{-(1+\mathrm{i})\hat{\eta}}\right\}\mathrm{e}^{\mathrm{i}(\theta+t)} - \epsilon^{1/3}\hat{R}_s^{1/3}\Omega_1\hat{\eta} + \ldots,$$

where B is to be determined. Continuity of velocity and shear stress at the gas–liquid interface now requires

$$A + B = 1 + \mathrm{i}, \qquad B = \delta A \quad \text{with} \quad \delta = \delta_\mu\delta_\nu^{-1/2}.$$

For a typical gas–liquid system, for example air and water, $\delta \ll 1$ and so $A = 1 + \mathrm{i} + O(\delta)$ and $B = O(\delta)$. The Stokes-layer solution is therefore unchanged at leading order in δ which in turn implies that the Reynolds stresses in the gas-phase Stokes layer, represented by the right-hand side of (22), are also unchanged at leading order in δ. Furthermore, in the liquid phase, the Reynolds stresses are $O(\delta^2)$ and therefore negligible. This means that the time-independent Stokes-layer solution at $O(\epsilon)$, namely (23), is unchanged and so Ω_1 is as given by (25). Finally, the solution in the interior that accommodates (23) is

$$\hat{\psi} = -\tfrac{1}{2}\epsilon^{1/3}\tilde{R}_s^{1/3}\Omega_1(r^2 - 1) + O(\epsilon),$$

https://doi.org/10.1017/S0022112003004312 Published online by Cambridge University Press

which is the counterpart of (21). This implies that at leading order within the liquid phase the liquid is in rigid-body rotation.

4. The spherical particle

As in the previous section, we begin our analysis with the case of a solid particle, now spherical. Subsequently we generalize to the case of a spherical droplet with large but finite viscosity, and in particular consider the internal circulation within it. Physically, this analysis will be appropriate for a liquid drop in a gas or a liquid medium of much lower viscosity. In order that a spherical shape may be maintained, it is necessary that the surface tension be sufficiently large. The case of a solid particle is then recovered by allowing the ratio of the coefficients of viscosity outside and inside the drop to tend to zero.

4.1. *A solid sphere*

The problem is now three-dimensional, and the simplification brought about by the introduction of a stream function for the two-dimensional flow of § 3 is not available. We must work with primitive variables, and the Navier–Stokes equations, (4), where $M^2 = \tilde{R}_s^{2/3}/\epsilon^{4/3}$. By analogy with (11) we expand the flow variables, now velocity and pressure, as

$$\boldsymbol{v} = \boldsymbol{v}_0^{(u)} + \epsilon^{1/3}\tilde{R}_s^{1/3}\boldsymbol{v}_1^{(s)} + \epsilon^{2/3}\tilde{R}_s^{-1/3}\boldsymbol{v}_2^{(u)} + \epsilon\{\boldsymbol{v}_3^{(s)} + \boldsymbol{v}_3^{(u)}\} + \epsilon^{4/3}\tilde{R}_s^{-2/3}\boldsymbol{v}_4^{(u)} + O(\epsilon^{5/3}), \quad (31)$$

$$p = p_0^{(u)} + \epsilon^{2/3}\tilde{R}_s^{-1/3}p_2^{(u)} + \epsilon\{p_3^{(s)} + p_3^{(u)}\} + \epsilon^{4/3}\tilde{R}_s^{-2/3}p_4^{(u)} + \epsilon^{5/3}\tilde{R}_s^{-1/3}\{p_5^{(s)} + p_5^{(u)}\} + O(\epsilon^2), \quad (32)$$

and similarly, as before, we write

$$\Omega = \epsilon^{1/3}\tilde{R}_s^{1/3}\Omega_1 + \epsilon\,\Omega_3 + O(\epsilon^{5/3}). \quad (33)$$

Substituting (31) and (32) into (4) gives, at leading order

$$\frac{\partial \boldsymbol{v}_0^{(u)}}{\partial t} = -\nabla p_0^{(u)}, \quad \nabla\cdot\boldsymbol{v}_0^{(u)} = 0,$$

from which we derive the irrotational-flow solution $\boldsymbol{v}_0^{(u)} = \{v_{0r}^{(u)}, v_{0\theta}^{(u)}, v_{0\phi}^{(u)}\}$, that satisfies $v_{0r}^{(u)} = 0$ at $r = 1$, and the far-field condition (5), as

$$\left.\begin{aligned} v_{0r}^{(u)} &= \left(1 - \frac{1}{r^3}\right)\sin\theta\,\mathrm{e}^{\mathrm{i}(t+\phi)}, \\ v_{0\theta}^{(u)} &= \left(1 + \frac{1}{2r^3}\right)\cos\theta\,\mathrm{e}^{\mathrm{i}(t+\phi)}, \\ v_{0\phi}^{(u)} &= \left(1 + \frac{1}{2r^3}\right)\mathrm{e}^{\mathrm{i}(t+\phi+\pi/2)}, \\ p_0^{(u)} &= \left(r + \frac{1}{2r^2}\right)\sin\theta\,\mathrm{e}^{\mathrm{i}(t+\phi-\pi/2)}. \end{aligned}\right\} \quad (34)$$

In (34), we have introduced spherical polar coordinates with $x = r\sin\theta\cos\phi$, $y = r\sin\theta\sin\phi$ and $z = r\cos\theta$. The x and y axes are along the vectors $\boldsymbol{i}$ and $\boldsymbol{j}$ in (5), while z is along the rotation axis.

Series complementary to (31) and (32) must again be introduced in the Stokes layer in order that conditions at the particle surface may be satisfied. Thus, in the Stokes

https://doi.org/10.1017/S0022112003004312 Published online by Cambridge University Press

layer we write

$$V_\theta = v_\theta, \quad V_\phi = v_\phi, \quad P = p, \quad V_\eta = \frac{\tilde{R}_s^{1/3}}{\sqrt{2}\,\epsilon^{2/3}} v_r, \quad \eta = \frac{\tilde{R}_s^{1/3}}{\sqrt{2}\,\epsilon^{2/3}}(r-1),$$

with expansions for $\{V_\eta, V_\theta, V_\phi\}$ and P as in (31) and (32).

In the Stokes layer, given that the pressure is constant across it, we have

$$\frac{\partial V_{0\theta}^{(u)}}{\partial t} = -\tfrac{3}{2}\cos\theta\, \mathrm{e}^{\mathrm{i}(t+\phi-\pi/2)} + \tfrac{1}{2}\frac{\partial^2 V_{0\theta}^{(u)}}{\partial \eta^2}.$$

The solution of this equation which satisfies the no-slip condition at $\eta = 0$, and matches with the corresponding outer solution in (34), is

$$V_{0\theta}^{(u)} = \tfrac{3}{2}\cos\theta \left\{1 - \mathrm{e}^{-(1+\mathrm{i})\eta}\right\} \mathrm{e}^{\mathrm{i}(t+\phi)}.$$

Similarly, we find

$$V_{0\phi}^{(u)} = \tfrac{3}{2} \left\{1 - \mathrm{e}^{-(1+\mathrm{i})\eta}\right\} \mathrm{e}^{\mathrm{i}(t+\phi+\pi/2)},$$

and, finally, from the continuity equation

$$V_{0\eta}^{(u)} = 3\,\sin\theta \left[\eta - \tfrac{1}{2}(1-\mathrm{i})\left\{1 - \mathrm{e}^{-(1+\mathrm{i})\eta}\right\}\right] \mathrm{e}^{\mathrm{i}(t+\phi)}.$$

Returning to the outer solution, the terms $O(\epsilon^{1/3})$ in (4) give, simply, $\nabla\cdot\boldsymbol{v}_1^{(s)} = 0$ whilst the terms $O(\epsilon^{2/3})$ give

$$\frac{\partial \boldsymbol{v}_2^{(u)}}{\partial t} = -\nabla p_2^{(u)}, \quad \nabla\cdot\boldsymbol{v}_2^{(u)} = 0.$$

This irrotational velocity field is driven by the displacement effect of the Stokes layer, represented by $V_{0\eta}^{(u)}$ above. We do not pursue it further. The terms $O(\epsilon)$ now yield

$$\frac{\partial \boldsymbol{v}_3^{(u)}}{\partial t} + \tfrac{1}{2}\nabla\left\{\boldsymbol{v}_0^{(u)}\cdot\boldsymbol{v}_0^{(u)}\right\} = -\nabla p_3^{(s)} - \nabla p_3^{(u)}, \quad \nabla\cdot\boldsymbol{v}_3^{(s)} = \nabla\cdot\boldsymbol{v}_3^{(u)} = 0,$$

which we regard as a system from which $p_3^{(u)}$, $p_3^{(s)}$ and $\boldsymbol{v}_3^{(u)}$, but not $\boldsymbol{v}_3^{(s)}$, may be determined. In particular, we find

$$p_3^{(s)} = \frac{3}{4r^3}\left(1 - \frac{1}{4r^3}\right)\sin^2\theta - \frac{1}{2}\left(1 + \frac{1}{r^3} + \frac{1}{4r^6}\right).$$

The terms $O(\epsilon^{4/3})$ give

$$\frac{\partial \boldsymbol{v}_4^{(u)}}{\partial t} + \tilde{R}_s\left\{\left(\boldsymbol{v}_0^{(u)}\cdot\nabla\right)\boldsymbol{v}_1^{(s)} + \left(\boldsymbol{v}_1^{(s)}\cdot\nabla\right)\boldsymbol{v}_0^{(u)}\right\} = -\nabla p_4^{(u)}, \quad \nabla\cdot\boldsymbol{v}_4^{(u)} = 0.$$

Since it is the steady streaming flow that is our prime concern, we retain from the terms at $O(\epsilon^{5/3})$ only those with a non-trivial time average to give

$$\tfrac{1}{2}\nabla\left\{2\left\langle\boldsymbol{v}_0^{(u)}\cdot\boldsymbol{v}_2^{(u)}\right\rangle + \tilde{R}_s\boldsymbol{v}_1^{(s)}\cdot\boldsymbol{v}_1^{(s)}\right\} - \tilde{R}_s\boldsymbol{v}_1^{(s)}\wedge\left[\nabla\wedge\boldsymbol{v}_1^{(s)}\right] = -\nabla p_5^{(s)} - \nabla\wedge\nabla\wedge\boldsymbol{v}_1^{(s)}. \quad (35)$$

Now, if we are not interested in determining the correction $p_5^{(s)}$ to the time-averaged pressure, we may write $\tilde{p}_5^{(s)} = p_5^{(s)} + \langle\boldsymbol{v}_0^{(u)}\cdot\boldsymbol{v}_2^{(u)}\rangle$, and (35) in the more familiar form

$$\tilde{R}_s\left(\boldsymbol{v}_1^{(s)}\cdot\nabla\right)\boldsymbol{v}_1^{(s)} = -\nabla\tilde{p}_5^{(s)} + \nabla^2\boldsymbol{v}_1^{(s)}, \quad \nabla\cdot\boldsymbol{v}_1^{(s)} = 0, \quad (36)$$

where we have included the already established continuity equation. We see that $\boldsymbol{v}_1^{(s)}$ satisfies the Navier–Stokes equations with $\tilde{R}_s$ as Reynolds number and $\tilde{p}_5^{(s)}$ adopting

https://doi.org/10.1017/S0022112003004312 Published online by Cambridge University Press

the role of the pressure. Equations (36) are, of course, the analogue of (20) for the case of the circular cylinder. The solution of (36) requires $\boldsymbol{v}_1^{(s)} \to 0$ as $r \to \infty$, but the condition at $r = 1$ can only be determined following a further consideration of the Stokes layer. The terms $O(\epsilon^{1/3})$ in the Stokes layer now yield

$$\frac{\partial^2 V_{1\theta}^{(s)}}{\partial \eta^2} = \frac{\partial^2 V_{1\phi}^{(s)}}{\partial \eta^2} = 0, \quad \frac{1}{\sin\theta}\frac{\partial}{\partial \theta}\left(\sin\theta\, V_{1\theta}^{(s)}\right) + \frac{\partial V_{1\eta}^{(s)}}{\partial \eta} = 0,$$

from which we infer, given the form of the angular velocity of the sphere in (33), that

$$V_{1\eta}^{(s)} = 0, \quad V_{1\theta}^{(s)} = 0, \quad V_{1\phi}^{(s)} = \Omega_1 \sin\theta, \tag{37}$$

where Ω_1 is undetermined. This result provides us immediately with the condition for $\boldsymbol{v}_1^{(s)}$, namely

$$v_{1r}^{(s)} = 0, \quad v_{1\theta}^{(s)} = 0, \quad v_{1\phi}^{(s)} = \Omega_1 \sin\theta \quad \text{at} \quad r = 1. \tag{38}$$

Returning to the Stokes layer, it is the terms driven by the Reynolds stresses that are now crucial in our development of the solution. These give the following, when time-averaged, and noting again that the pressure is uniform across the Stokes layer,

$$\frac{1}{2}\frac{\partial^2 V_{3\theta}^{(s)}}{\partial \eta^2} = \tfrac{9}{16}\sin 2\theta + \left\langle V_{0\eta}^{(u)}\frac{\partial V_{0\theta}^{(u)}}{\partial \eta} + V_{0\theta}^{(u)}\frac{\partial V_{0\theta}^{(u)}}{\partial \theta} + \frac{V_{0\phi}^{(u)}}{\sin\theta}\frac{\partial V_{0\theta}^{(u)}}{\partial \phi} - V_{0\phi}^{(u)2}\cot\theta \right\rangle, \tag{39}$$

$$\frac{1}{2}\frac{\partial^2 V_{3\phi}^{(s)}}{\partial \eta^2} = \left\langle V_{0\eta}^{(u)}\frac{\partial V_{0\phi}^{(u)}}{\partial \eta} + V_{0\theta}^{(u)}\frac{\partial V_{0\phi}^{(u)}}{\partial \theta} + \frac{V_{0\phi}^{(u)}}{\sin\theta}\frac{\partial V_{0\phi}^{(u)}}{\partial \phi} + V_{0\theta}^{(u)}V_{0\phi}^{(u)}\cot\theta \right\rangle. \tag{40}$$

The solutions of (39), (40) may be written as

$$V_{3\theta}^{(s)} = \tfrac{9}{8}\sin 2\theta\left(\eta \mathrm{e}^{-\eta}\cos\eta - \eta \mathrm{e}^{-\eta}\sin\eta - \mathrm{e}^{-\eta}\cos\eta - 3\mathrm{e}^{-\eta}\sin\eta - \tfrac{1}{4}\mathrm{e}^{-2\eta} + \tfrac{5}{4}\right) + K_\theta(\theta) + \left.\frac{\partial v_{1\theta}^{(s)}}{\partial r}\right|_{r=1}\sqrt{2}\,\eta, \tag{41}$$

$$V_{3\phi}^{(s)} = \tfrac{9}{8}\sin\theta\left(2\eta \mathrm{e}^{-\eta}\cos\eta + 2\eta \mathrm{e}^{-\eta}\sin\eta + 4\mathrm{e}^{-\eta}\cos\eta - 2\mathrm{e}^{-\eta}\sin\eta - \mathrm{e}^{-2\eta} - 3\right) + K_\phi(\theta) + \left.\frac{\partial v_{1\phi}^{(s)}}{\partial r}\right|_{r=1}\sqrt{2}\,\eta, \tag{42}$$

where K_θ and K_ϕ are arbitrary functions, independent of ϕ in view of the expected rotational symmetry of the steady streaming, and the last term in each of (41) and (42) is required in order to provide a satisfactory match with the outer solution. For the case of a solid sphere, the no-slip condition simply yields

$$K_\theta = 0, \qquad K_\phi = \Omega_3 \sin\theta. \tag{43}$$

We are now in a position to calculate the tangential stress components at the particle surface. Denoting by $\tau_{r\theta}$ and $\tau_{r\phi}$ the dimensionless θ and ϕ components such that

$$\tau_{r\theta} = \frac{1}{\epsilon}\left(\frac{1}{\sqrt{2}}\frac{\partial V_\theta^{(s)}}{\partial \eta} - \frac{\epsilon^{2/3}}{\tilde{R}_s^{1/3}}V_\theta^{(s)}\right)\Bigg|_{\eta=0}, \quad \tau_{r\phi} = \frac{1}{\epsilon}\left(\frac{1}{\sqrt{2}}\frac{\partial V_\phi^{(s)}}{\partial \eta} - \frac{\epsilon^{2/3}}{\tilde{R}_s^{1/3}}V_\phi^{(s)}\right)\Bigg|_{\eta=0},$$

https://doi.org/10.1017/S0022112003004312 Published online by Cambridge University Press

at leading order we then find

$$\tau_{r\theta} = \left(\frac{1}{\sqrt{2}} \frac{\partial V_{3\theta}^{(s)}}{\partial \eta} - V_{1\theta}^{(s)} \right) \Bigg|_{\eta=0}, \quad \tau_{r\phi} = \left(\frac{1}{\sqrt{2}} \frac{\partial V_{3\phi}^{(s)}}{\partial \eta} - V_{1\phi}^{(s)} \right) \Bigg|_{\eta=0}$$

which gives, using (37), (38), (41) and (42),

$$\tau_{r\theta} = \left(\frac{\partial v_{1\theta}^{(s)}}{\partial r} - v_{1\theta}^{(s)} \right) \Bigg|_{r=1} - \frac{9}{16\sqrt{2}} \sin 2\theta, \quad \tau_{r\phi} = \left(\frac{\partial v_{1\phi}^{(s)}}{\partial r} - v_{1\phi}^{(s)} \right) \Bigg|_{r=1} - \frac{9}{4\sqrt{2}} \sin \theta. \quad (44)$$

Each of (44) consists of two parts, the first of which is the viscous stress due to the leading-order outer steady flow. The second part is present whether the sphere is fixed or allowed to rotate freely; it can be interpreted as an acoustic stress, and our result is a particular case of Lee & Wang (1989), who considered a more general case for a fixed sphere. We note that the dimensional value of the stresses is obtained by multiplying (44) by $\rho U_0^2 \epsilon^{2/3} \tilde{R}_s^{-1/3}$.

With the stresses given by (44), we can now calculate the net torque on the sphere as

$$\Gamma = \Gamma_{vis} + \Gamma_{ac}, \quad (45)$$

where

$$\Gamma_{vis} = 2\pi \int_0^{\pi} \left(\frac{\partial v_{1\phi}^{(s)}}{\partial r} - v_{1\phi}^{(s)} \right) \Bigg|_{r=1} \sin^2 \theta \, \mathrm{d}\theta, \qquad \Gamma_{ac} = -3\sqrt{2}\pi,$$

which is the counterpart of (24). Again, we note that the dimensional value of the torque is restored by multiplying (45) by $\rho U_0^2 a^3 \epsilon^{2/3} \tilde{R}_s^{-1/3}$. The two terms in (45) are the viscous torque due to the particle rotation, and the acoustic torque.

The problem for $\boldsymbol{v}_1^{(s)}$ and Ω_1 is now fully determined. We have equations (36) and boundary conditions (38), together with the condition that $\boldsymbol{v}_1^{(s)} \to 0$ as $r \to \infty$, and that the net torque in (45) vanishes, i.e. $\Gamma = 0$.

For $\tilde{R}_s \ll 1$, the solution is straightforward:

$$v_{1r}^{(s)} = 0, \quad v_{1\theta}^{(s)} = 0, \quad v_{1\phi}^{(s)} = \frac{\Omega_1 \sin \theta}{r^2}, \quad (46)$$

with

$$\Omega_1 = -\frac{3}{4\sqrt{2}},$$

and may be compared with the circular cylinder result (21) and (25).

For larger values of $\tilde{R}_s$, we can take advantage of earlier work; for example Takagi (1977) has obtained the viscous torque on a rotating sphere in the form of a seven-term series in powers of Reynolds number, Re, whilst Dennis *et al.* (1981) have found solutions of the Navier–Stokes equations and the torque numerically for $Re = O(1)$, and Banks (1976) has obtained them for $Re \gg 1$. In the latter case, the flow over the sphere assumes a classical boundary-layer character. To establish a correspondence with these earlier studies, we scale the velocity component with Ω_1, and so normalize the condition (38) at $r = 1$. This then identifies the Reynolds number of the earlier work with $|\Omega_1| \tilde{R}_s$. Dennis *et al.* present numerical values of the viscous torque on the sphere, represented by the first term in (45). In our formulation their result can be written as

$$\Gamma_{vis} = -\Omega_1 \, f(|\Omega_1| \tilde{R}_s), \quad (47)$$

https://doi.org/10.1017/S0022112003004312 Published online by Cambridge University Press

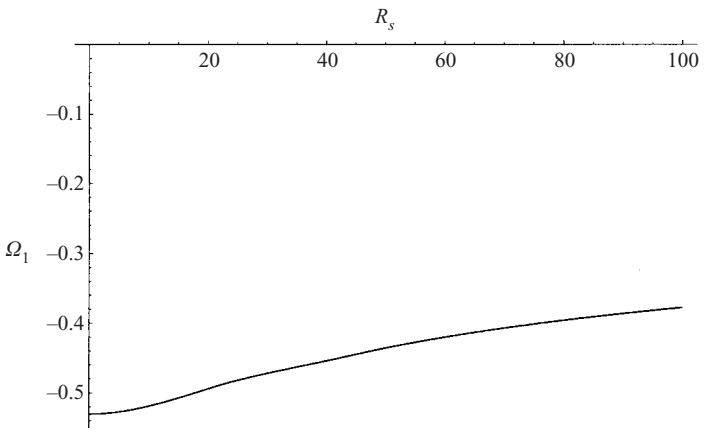


FIGURE 2. The rotation rate of a spherical particle *vs.* the streaming Reynolds number.

where the function $f(Re)$ is derivable from Dennis *et al.* (1981). Then, from (45) and (47) we can calculate $\Omega_1 = \Omega_1(\tilde{R}_s)$. For large Reynolds numbers, Banks (1976) has established $f(Re) = 3.24Re^{1/2}$, so that (45) and (47) yield $\Omega_1 = -2.57\tilde{R}_s^{-1/3}$ for $\tilde{R}_s \gg 1$. In fact, Dennis *et al.* have proposed a correction to the results of Banks such that $f(Re) = 3.24Re^{1/2} + 15.5$, which agrees with their numerical computations within 2% for $Re > 20$. Then, from (45) and (47), we obtain

$$\left(3.24|\Omega_1|^{1/2}\tilde{R}_s^{1/2} + 15.5\right)\Omega_1 = -3\sqrt{2}\pi,$$

which is used to determine Ω_1, provided that $|\Omega_1|\,\tilde{R}_s > 20$. In figure 2, we show $\Omega_1 = \Omega_1(\tilde{R}_s)$. Note that, as in the case of a circular cylinder, the sphere rotates in the same direction as the distant velocity vector (5).

It is instructive to rewrite the results for $\tilde{R}_s \ll 1$ and $\tilde{R}_s \gg 1$ in terms of Ω in equation (33). We have

$$\Omega = -\frac{3}{4\sqrt{2}}(\epsilon\,\tilde{R}_s)^{1/3} \quad \text{for} \quad \tilde{R}_s \ll 1, \qquad \Omega = -2.57\,\epsilon^{1/3} \quad \text{for} \quad \tilde{R}_s \gg 1$$

which can be compared with (26) in the cylinder case. While (26) holds in a broad range of $\tilde{R}_s$, from $\tilde{R}_s = 0$ well into $\tilde{R}_s \gg 1$, in the sphere case we obtain a different scaling for $\tilde{R}_s \gg 1$. This is due to the outer boundary-layer structure being absent in the cylinder case, where the line vortex is the exact solution even at $\tilde{R}_s \gg 1$. As a consequence, for a sphere we always have $|\Omega| \ll 1$ as long as $\epsilon \ll 1$, i.e. the rotation velocity is much smaller than the velocity scale of the primary oscillatory flow. On the contrary, in the cylinder case with $\tilde{R}_s \gg 1$ we can in principle achieve $|\Omega| = O(1)$ or even $|\Omega| \gg 1$, despite ϵ still being small. This is what led us to the asymptotic case treated at the end of § 3.1.

At this point it is both interesting and instructive to return to the case $\tilde{R}_s \ll 1$. From (46) we recall that the outer flow is dominated by the azimuthal, or swirling, component of velocity. From (36) we may infer that corrections to this will be $O(\tilde{R}_s)$, and such terms will dominate the meridional flow; accordingly we write $\boldsymbol{v}^{(s)} = \boldsymbol{v}_{10}^{(s)} + \tilde{R}_s\boldsymbol{v}_{11}^{(s)} + \ldots$ where the leading term $\boldsymbol{v}_{10}^{(s)}$ is as in (46). Another contribution to the meridional flow is given by $\boldsymbol{v}_3^{(s)}$ which is instigated by the effective slip velocity, which by matching with (41) and taking into account (43) can be written as

$$v_{3\theta}^{(s)} = \tfrac{45}{32}\sin 2\theta \quad \text{at} \quad r = 1.$$

https://doi.org/10.1017/S0022112003004312 Published online by Cambridge University Press

From the expansion (31), we see that these contributions to the outer meridional flow will be comparable if $\tilde{R}_s = O(\epsilon^{1/2})$. To pursue this distinguished limit let us formally set $\tilde{R}_s = \epsilon^{1/2} R$ where $R = O(1)$. Now, it can be shown that for small $\tilde{R}_s$, the velocity field $\boldsymbol{v}_3^{(s)}$ satisfies Stokes' equations and further, since the meridional flow is axisymmetric, we may introduce the Stokes streamfunction with

$$R^{4/3} v_{11r}^{(s)} + v_{3r}^{(s)} = \frac{1}{r^2 \sin\theta} \frac{\partial \tilde{\psi}_3^{(s)}}{\partial \theta}, \quad R^{4/3} v_{11\theta}^{(s)} + v_{3\theta}^{(s)} = -\frac{1}{r \sin\theta} \frac{\partial \tilde{\psi}_3^{(s)}}{\partial r}, \tag{48}$$

so that $\tilde{\psi}_3^{(s)}$ satisfies

$$\left\{ \frac{\partial^2}{\partial r^2} + \frac{\sin\theta}{r^2} \frac{\partial}{\partial \theta} \left(\frac{1}{\sin\theta} \frac{\partial}{\partial \theta} \right) \right\}^2 \tilde{\psi}_3^{(s)} = -\frac{27}{16} \frac{R^{4/3}}{r^5} \sin^2\theta \cos\theta. \tag{49}$$

The boundary conditions are

$$\tilde{\psi}_3^{(s)} \sim o(r^2) \ \text{ as } \ r \to \infty, \quad \tilde{\psi}_3^{(s)} = 0, \quad \frac{\partial \tilde{\psi}_3^{(s)}}{\partial r} = -\tfrac{45}{16} \sin^2\theta \cos\theta \ \text{ at } \ r = 1. \tag{50}$$

The solution of (49) and (50) is, then,

$$\tilde{\psi}_3^{(s)} = \tfrac{9}{256} R^{4/3} \left(\frac{2}{r} - \frac{1}{r^2} - 1 \right) \sin^2\theta \cos\theta + \tfrac{45}{32} \left(\frac{1}{r^2} - 1 \right) \sin^2\theta \cos\theta. \tag{51}$$

The first term of (51) may be identified with the 'centrifugal' effect about the rotating sphere, whilst the second is associated with the effective slip velocity. It is interesting to note that this latter term has the same structure as the outer streaming in the case of single-axis oscillations of a sphere studied by Riley (1966), except that the sign differs. In the present bi-axial situation, the θ-component of the flow is directed from the symmetry axis to the equator, in the single-axis case the reverse is true.

4.2. *A liquid drop*

We now generalize the results obtained above to the case of a drop, assuming that the ratio of the viscosities outside and inside the drop is small. An important prototype has the liquid drop in a gaseous medium; and the solid-particle case corresponds to $\delta_\mu = 0$. We assume that the surface tension is strong enough to maintain the time-averaged drop shape nearly spherical.

The steady flow inside the drop is induced by the surface tangential stresses. As has been pointed out in § 3.2, the penetration of the primary oscillatory flow into the drop is negligible in the present case. Therefore, the expressions (44) remain unchanged to leading order.

In view of the relatively high coefficient of viscosity inside the drop, we would expect the tangential stress to be entirely taken up by the internal flow, with the influence of the outer medium negligible. However, this is not the case when the net torque due to the stresses is not zero, for the internal flow in a rotationally symmetric drop can never compensate for the net torque. It has rather to be compensated by the outer fluid motion. As a result, the flow inside the drop is a superposition of a relatively strong rigid-body rotation (the only possible flow that exerts no viscous stress on the surface from inside) with velocity $O(\epsilon^{1/3} \tilde{R}_s^{1/3} U_0)$ and a relatively weak internal circulation with velocity $O(\epsilon^{1/3} \tilde{R}_s^{1/3} \delta_\mu U_0)$. Here, the velocity scales are given assuming the Reynolds numbers of order unity.

https://doi.org/10.1017/S0022112003004312 Published online by Cambridge University Press

For the velocity and pressure fields within the droplet we introduce non-dimensional variables, analogous to (3), as

$$\hat{\boldsymbol{v}}' = U_0 \hat{\boldsymbol{v}}, \quad \hat{p}' = \hat{\rho} a \omega U_0 \hat{p}.$$

Our main concern is with the steady streaming within the droplet; we write the time-averaged flow variables, retaining a similar notation to that used previously in the region beyond the particle, as

$$\langle \hat{\boldsymbol{v}} \rangle = \Omega\, \boldsymbol{k} \wedge \boldsymbol{x} + \epsilon M_\mu \{ \hat{\boldsymbol{v}}_3^{(s)} + \epsilon^{2/3} \tilde{R}_s^{-1/3} \hat{\boldsymbol{v}}_5^{(s)} + O(\epsilon^{4/3}) \}, \tag{52}$$

$$\langle \hat{p} \rangle = \tfrac{1}{2} \epsilon\, \Omega^2 r^2 \sin^2\theta + \epsilon M_\mu \delta_\nu^{-1} \{ \epsilon^{4/3} \tilde{R}_s^{-2/3} \hat{p}_7^{(s)} + O(\epsilon^2) \}, \tag{53}$$

where $\boldsymbol{k}$ is the unit vector along the rotation axis $\theta = 0$ and Ω is again of the form (33). We recall that the parameters M_μ and δ_ν are treated as $O(1)$ quantities; this minimizes the number of asymptotic orders involved in (52) and (53). Since the oscillatory component of flow is asymptotically small there is no contribution to the pressure at $O(\epsilon)$, i.e. $\hat{p}_3^{(s)} \equiv 0$, and that which is $O(\epsilon^{5/3})$ is embodied in the leading term of (53).

Introducing (52) and (53) into the Navier–Stokes equations, with Ω as in (33), and retaining only the leading-order terms, yields

$$2 \tilde{R}_s \delta_\nu \Omega_1\, \boldsymbol{k} \wedge \hat{\boldsymbol{v}}_3^{(s)} = -\nabla \hat{p}_7^{(s)} + \nabla^2 \hat{\boldsymbol{v}}_3^{(s)}, \quad \nabla \cdot \hat{\boldsymbol{v}}_3^{(s)} = 0. \tag{54a, b}$$

Equation (54*a*) is essentially a linearization of the momentum equation around a rigid-body rotation. It has been taken into account that the velocity components are independent of ϕ. Thus the left-hand side reduces to the Coriolis term. We see that $\tilde{R}_s \delta_\nu$ plays the role of the Reynolds number for the internal circulation.

The boundary conditions for (54) are, from continuity of stress and non-penetration,

$$\frac{\partial \hat{v}_{3\theta}^{(s)}}{\partial r} - \hat{v}_{3\theta}^{(s)} = \tau_{r\theta}, \quad \frac{\partial \hat{v}_{3\phi}^{(s)}}{\partial r} - \hat{v}_{3\phi}^{(s)} = \tau_{r\phi}, \quad \hat{v}_{3r}^{(s)} = 0 \qquad \text{at} \quad r = 1, \tag{55}$$

where, in (55), the quantities $\tau_{r\theta}$, $\tau_{r\phi}$ are as in (44). At this stage they, as well as Ω_1, are regarded as fully known, for the solution of the outer problem about the flow around a sphere in a solid-body rotation is presumed to be known. We note that, in view of the condition $\Gamma = 0$ in (45), the net torque due to the tangential stresses in (55) vanishes. Therefore the interior problem (54) and (55) is resolvable. Thus equations (54) and (55) constitute the formulation for the recirculating flow inside the droplet.

To complete the solution (41) and (42) for this case of a droplet we have, from the continuity of velocity at the interface,

$$K_\theta = M_\mu \hat{v}_{3\theta}^{(s)}\big|_{r=1}, \quad K_\phi = M_\mu \hat{v}_{3\phi}^{(s)}\big|_{r=1} + \Omega_3 \sin\theta \tag{56}$$

and we note that the parameter M_μ provides a measure of the effect of drop liquidity on the outer streaming.

To proceed, we now consider the situation for $\tilde{R}_s \ll 1$. The outer solution is then given by (46) so that we now have, in (55),

$$\tau_{r\theta} = -\frac{9}{16\sqrt{2}} \sin 2\theta, \quad \tau_{r\phi} = 0.$$

https://doi.org/10.1017/S0022112003004312 Published online by Cambridge University Press

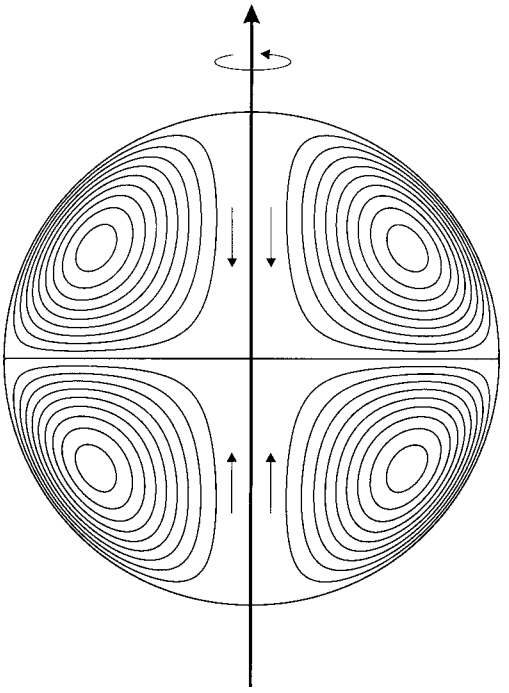


FIGURE 3. Internal circulation within a rotating drop.
The arrows indicate direction of the flow.

It then follows that $\hat{v}_{3\phi}^{(s)} = 0$. The resulting axisymmetric flow may be expressed in terms of a streamfunction $\hat{\psi}_3^{(s)}$ with

$$\hat{v}_{3r}^{(s)} = \frac{1}{r^2 \sin\theta}\frac{\partial \hat{\psi}_3^{(s)}}{\partial \theta}, \quad \hat{v}_{3\theta}^{(s)} = -\frac{1}{r \sin\theta}\frac{\partial \hat{\psi}_3^{(s)}}{\partial r},$$

which satisfies the homogeneous form of equation (49) with solution

$$\hat{\psi}_3^{(s)} = \frac{9}{80\sqrt{2}}(r^5 - r^3)\sin^2\theta\,\cos\theta. \tag{57}$$

The streamlines associated with (57) are shown in figure 3. We see that the internal circulation within the drop, over and above the rigid-body rotation, takes the form of two toroidal vortices whose common axis coincides with the axis of rotation. There is a striking similarity between this case and the internal streaming within a droplet subjected to single-axis oscillations (Yarin *et al.* 1999; Zhao *et al.* 1999*b*). There the structure of the internal circulation is exactly as in (57), but the flow is in the opposite direction. These similarities are, of course, confined to the situation for which $\tilde{R}_s \ll 1$.

As with the solid particle, we are now able to consider the meridional flow in the outer streaming, for the case $\tilde{R}_s = O(\epsilon^{1/2})$, and in particular the modification brought about by the internal circulation within the drop. Proceeding as in (48), $\tilde{\psi}_3^{(s)}$ again satisfies equation (49), but from (56) and (57) we have $K_\theta = -(9M_\mu/40\sqrt{2})\sin\theta\cos\theta$, and for the solution to match satisfactorily with the Stokes-layer solution (41), we must now have, in (50),

$$\frac{\partial \tilde{\psi}_3^{(s)}}{\partial r} = -\left(\frac{45}{16} - \frac{9}{40\sqrt{2}}M_\mu\right)\sin^2\theta\cos\theta \quad \text{at} \quad r = 1.$$

https://doi.org/10.1017/S0022112003004312 Published online by Cambridge University Press

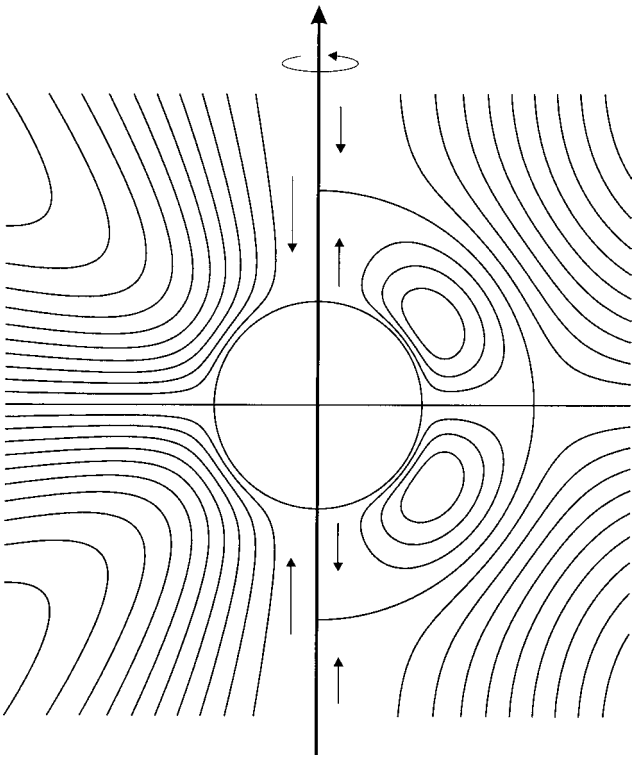


FIGURE 4. Meridional flow outside a rotating spherical particle, equation (58). On the left-hand side, the parameters are $M_\mu = 0$ (solid sphere), $R = 10$. On the right-hand side, we have $M_\mu = 21$ (a drop) and $R = 10$.

The appropriate solution is then

$$\tilde{\psi}_3^{(s)} = \tfrac{9}{256} R^{4/3} \left(\frac{2}{r} - \frac{1}{r^2} - 1 \right) \sin^2\theta \cos\theta + \left(\frac{45}{32} - \frac{9}{80\sqrt{2}} M_\mu \right) \left(\frac{1}{r^2} - 1 \right) \sin^2\theta \cos\theta. \tag{58}$$

Again we note that the second term of (58) is, but for a change of sign, identical to the outer streaming obtained by Zhao *et al.* (1999*b*) in the case of single-axis oscillations of a drop. We may note that, for sufficiently large M_μ, $\tilde{\psi}_3^{(s)}$ will change sign as $r \to 1$, with the implication that on each hemisphere there is a recirculation of the outer flow close to the drop.

In figure 4, we show two examples of this outer streaming. To the left of the axis of rotation, we have streamlines for $R = 10$, $M_\mu = 0$, the case of a solid sphere, when (58) reduces to (51), whilst to the right of that axis streamlines for $M_\mu = 21$ and, again, $R = 10$. In the latter case the 'liquidity' of the droplet manifests itself by regions of closed streamlines which are, of course, sections of toroidal vortices.

5. Conclusions

In this paper, we have shown how suitable orthogonal acoustic beams may rotate levitated solid or liquid particles, which we have taken in the nature of circular cylinders and spheres. In the case of liquid particles, their coefficient of viscosity was

https://doi.org/10.1017/S0022112003004312 Published online by Cambridge University Press

assumed large as compared to the outside fluid. In particular, we have identified an appropriate Reynolds number for the time-averaged flow, which differs from that associated with particles that are fixed. For the case of a cylinder, the rotation rate may become sufficiently large that steady streaming velocities in excess of the velocity amplitude of the primary oscillations are realized. For a sphere, the induced time-averaged flow is more complex, and speeds associated with it always remain small compared with the velocity amplitude of the oscillations. The case of a liquid sphere differs from that of a liquid cylinder, for whilst both rotate essentially as a solid body there is, within the liquid sphere, a superimposed recirculation which, in turn, influences the streaming beyond it.

The authors are grateful to K. Ohsaka for helpful discussions of experimental possibilities for inducing an acoustic torque on levitated particles, and to NASA and the Leverhulme Trust for financial support.

REFERENCES

Banks, W. H. H. 1976 The laminar boundary layer on a rotating sphere. *Acta. Mech.* **24**, 273–287.

Dennis, S. C. R., Ingham, D. B. & Singh, S. H. 1981 The steady flow of a viscous fluid due to a rotating sphere. *Q. J. Mech. Appl. Maths* **34**, 361–381.

Lee, C. P. & Wang, T. G. 1989 Near-boundary streaming around a small sphere due to two orthogonal standing waves. *J. Acoust. Soc. Am.* **85**, 1081–1088.

Lee, C. P. & Wang, T. G. 1990 Outer acoustic streaming. *J. Acoust. Soc. Am.* **88**, 2367–2375.

Rhim, W. K., Chung, S. & Elleman, D. 1988 Experiments on rotating charged liquid drops. *AIP Conf. Proc. 197, Drops and Bubbles, Third International Colloquium* (ed. T. G. Wang), Monterey, CA.

Riley, N. 1966 On a sphere oscillating in a viscous fluid. *Q. J. Mech. Appl. Maths* **19**, 461–472.

Riley, N. 1967 Oscillatory viscous flows: review and extension. *J. Inst. Math. Applics.* **3**, 419–434.

Riley, N. 1992 Acoustic streaming about a cylinder in orthogonal beams. *J. Fluid Mech.* **242**, 387–394.

Takagi, H. 1977 Viscous flow induced by slow rotation of a sphere. *J. Phys. Soc. Japan* **42**, 319–325.

Yarin, A. L., Brenn, G., Kastner, O., Rensink, D. & Tropea, C. 1999 Evaporation of acoustically levitated droplets. *J. Fluid Mech.* **399**, 151–204.

Zhao, H., Sadhal, S. S. & Trinh, E. H. 1999*a* Singular perturbation analysis of an acoustically levitated sphere: flow about the velocity node. *J. Acoust. Soc. Am.* **106**, 589–595.

Zhao, H., Sadhal, S. S. & Trinh, E. H. 1999*b* Internal circulation in a drop in an acoustic field. *J. Acoust. Soc. Am.* **106**, 3289–3295.

https://doi.org/10.1017/S0022112003004312 Published online by Cambridge University Press